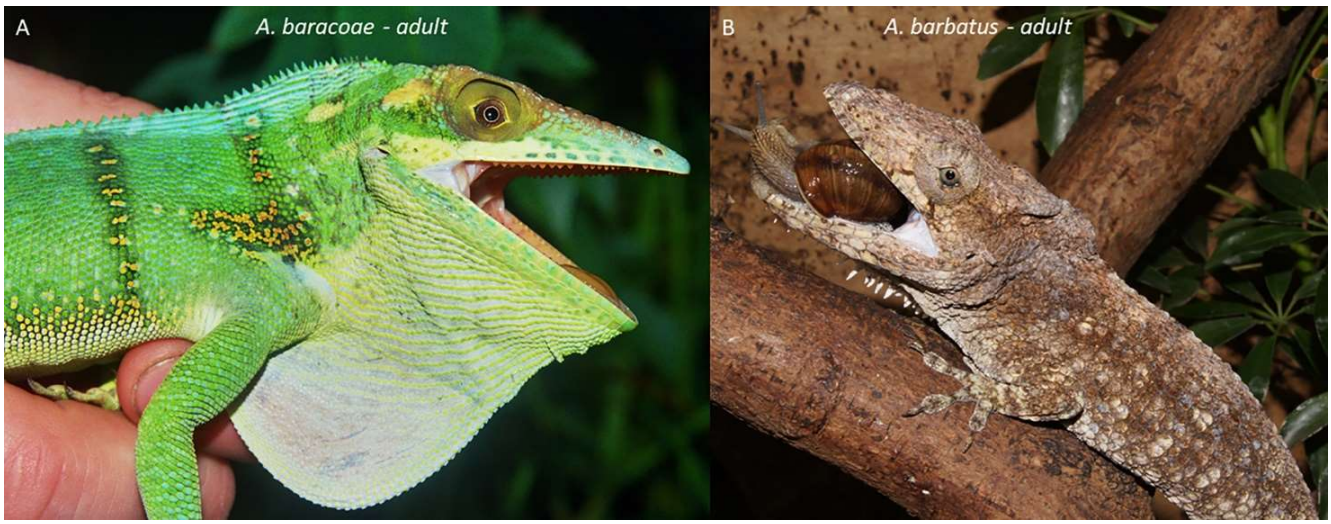


Fig. S1. Shows pictures of adult *A. baracoae* (A) and *A. barbatus* (B), a member of the Cuban false chameleons. *A. baracoae* has a slender head and long limbs (A), while *A. barbatus*, shown eating a snail, has massive jaws and short limbs (B).

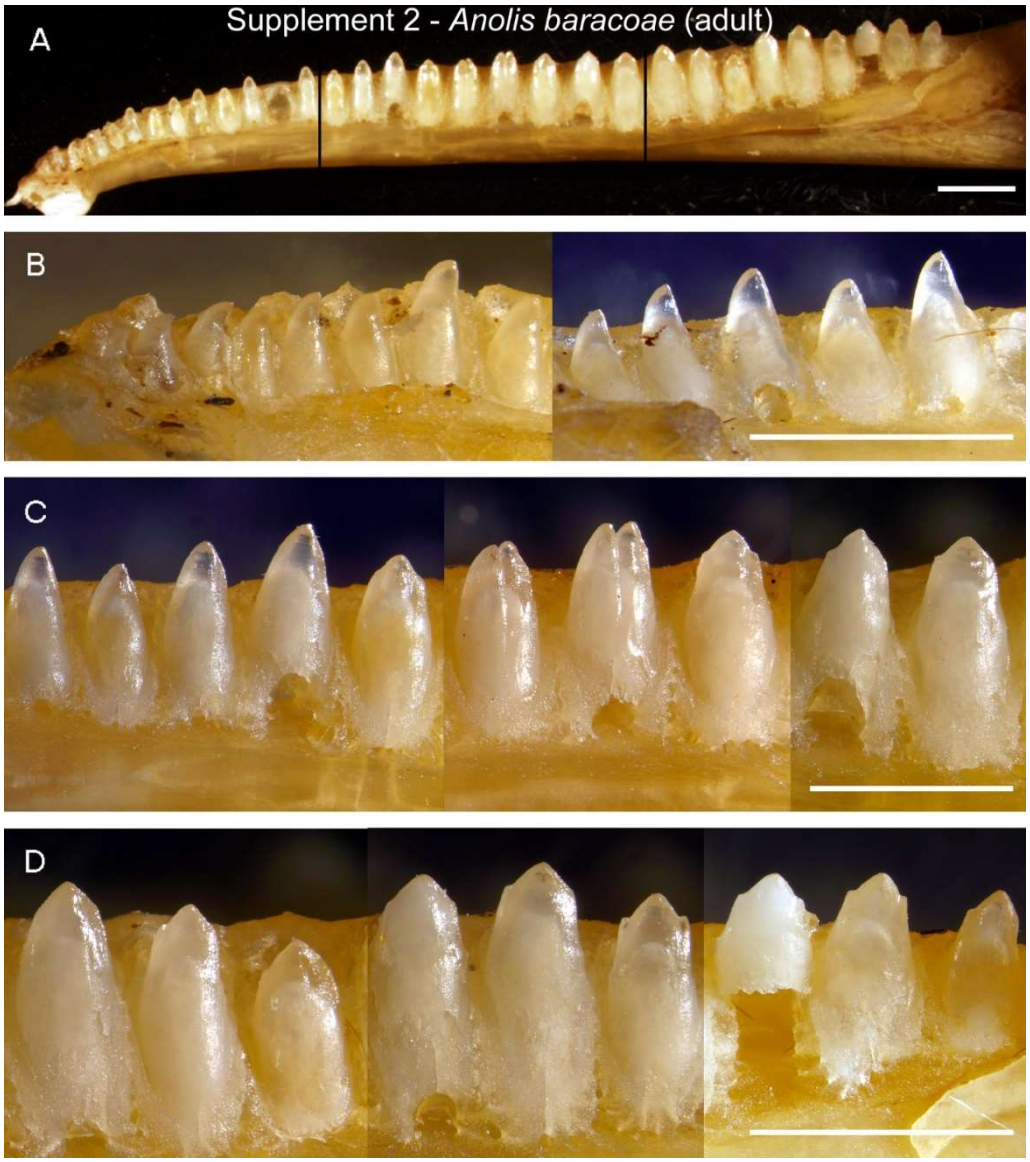


Fig. S2. Light microscope photograph of the adult dentition of *A. baracoae*. Image (A) shows the lower jaw from the lingual side. The black vertical lines separate the lower jaw into rostral, middle and caudal segments. Images (B, C, D) show enlarged view of the dentition. The size of scale bars is 2 mm.

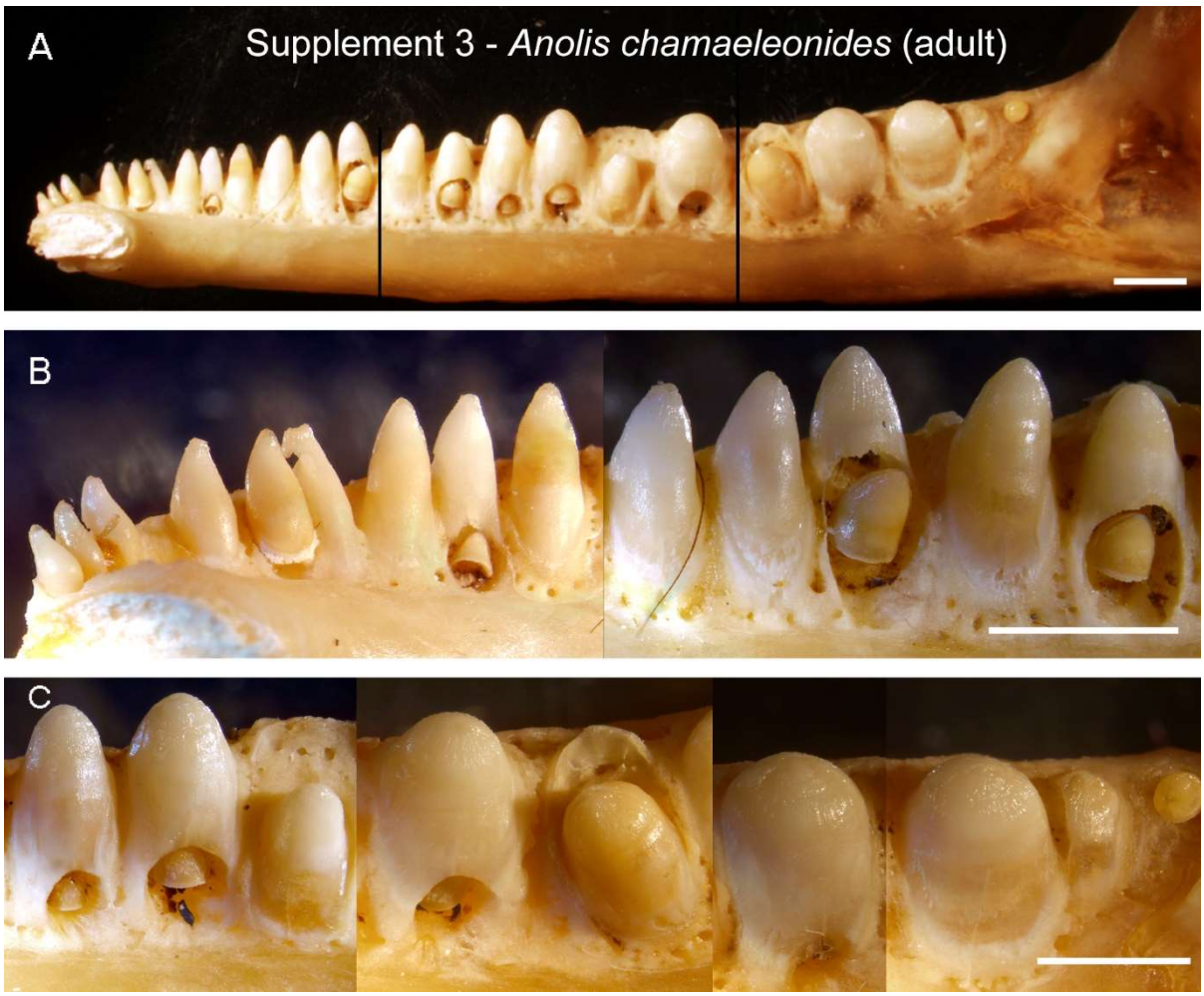


Fig. S3. Light microscope photograph of the adult dentition of *A. chamaeleonides*. Image (A) shows the lower jaw from the lingual side. The black vertical lines divide the lower jaw into rostral, middle, and caudal segments. Images (B, C) provide an enlarged view of the dentition. The scale bars are 2 mm in size.

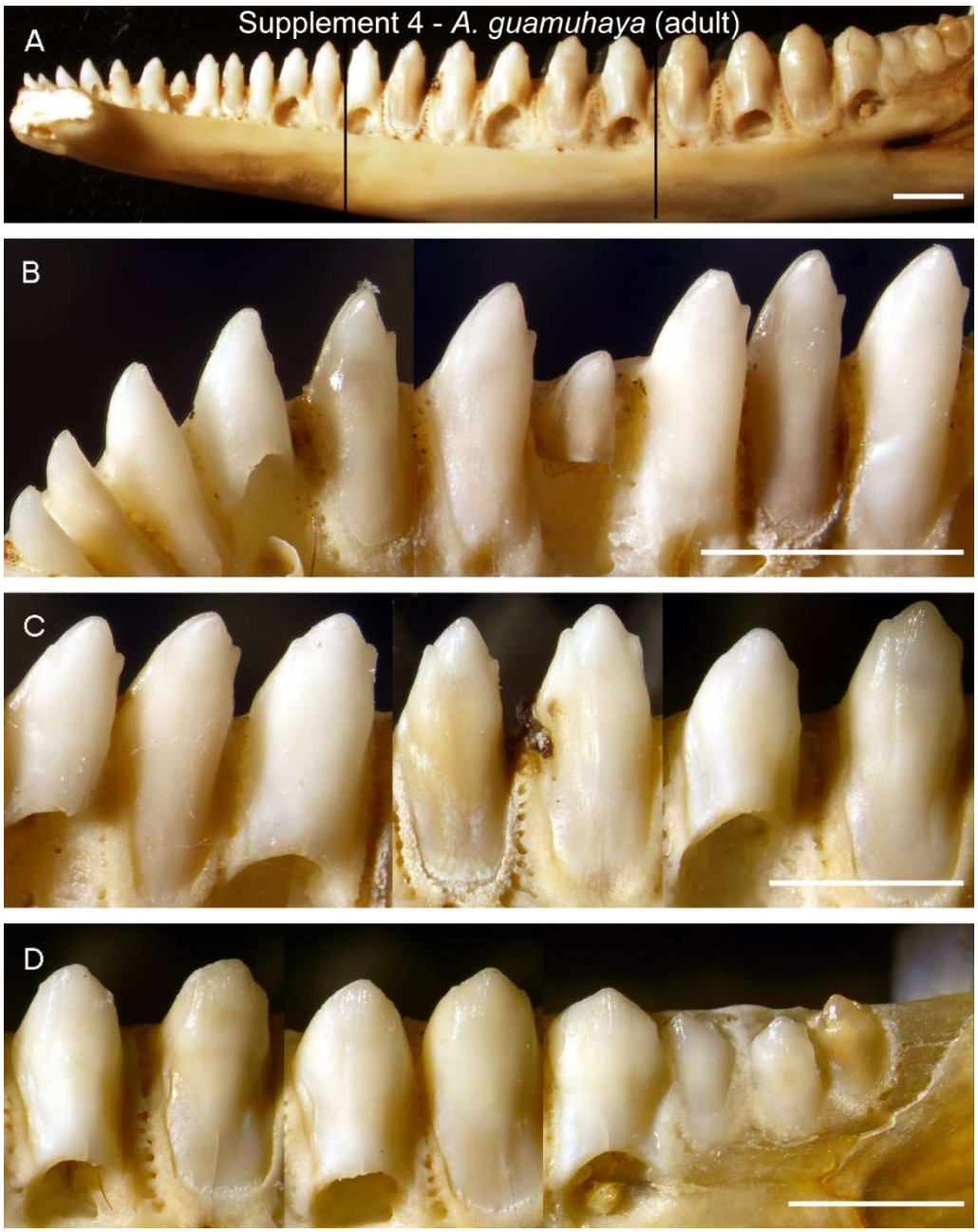


Fig. S4. Light microscope photograph of the adult dentition of *A. guamuhaya*. Image (A) shows the lower jaw from the lingual side. The black vertical lines divide the lower jaw into rostral, middle, and caudal segments. Images (B, C, D) provide an enlarged view of the dentition. The scale bars are 2 mm in size.

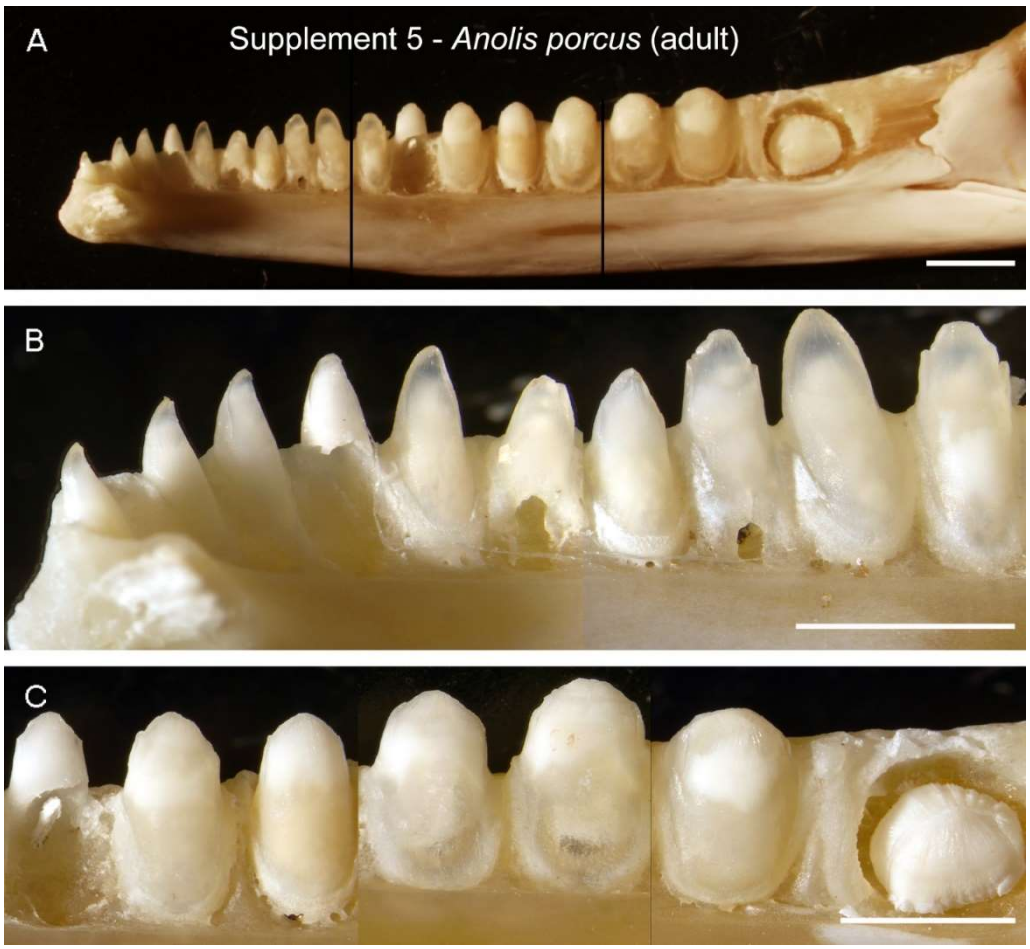


Fig. S5. Light microscope photograph of the adult dentition of *A. porcus*. Image (A) shows the lower jaw from the lingual side. The black vertical lines separate the lower jaw into rostral, middle, and caudal segments. Images (B, C) show enlarged views of the dentition. The scale bars are 2 mm.

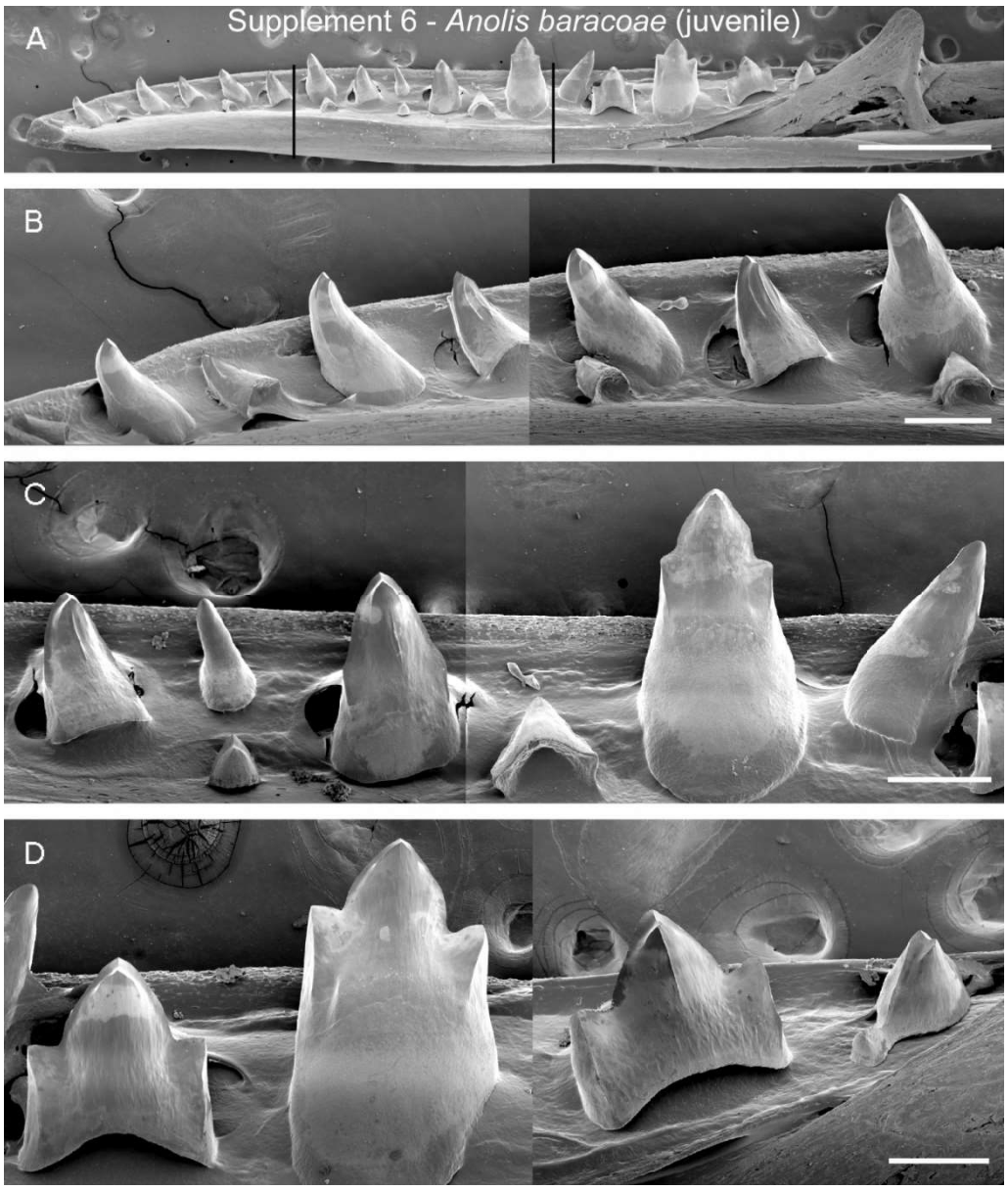


Fig. S6. SEMs of the juvenile dentition of *A. baracoae*. Image (A) shows the lower jaw from the lingual side with a scale bar of 1 mm. The black vertical lines divide the lower jaw into rostral, middle, and caudal segments. Images (B, C, D) provide an enlarged view of the dentition with scale bars of 0.2 mm.

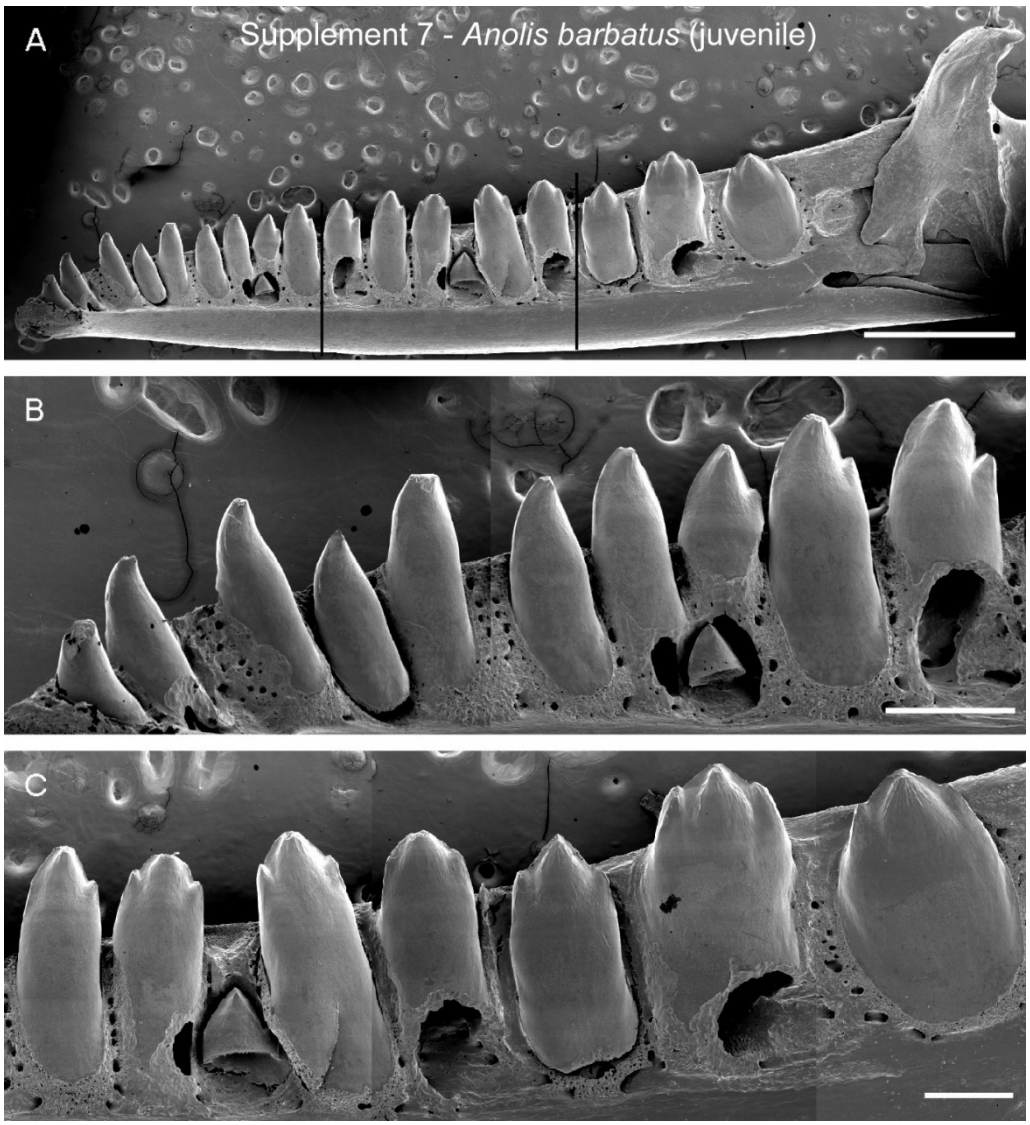


Fig. S7. SEMs of the juvenile dentition of *A. barbatus*. Image (A) shows the lower jaw from the lingual side, with a scale bar of 2 mm. The black vertical lines divide the lower jaw into rostral, middle, and caudal segments. Images (B, C) provide an enlarged view of the dentition, with scale bars of 0.5 mm.

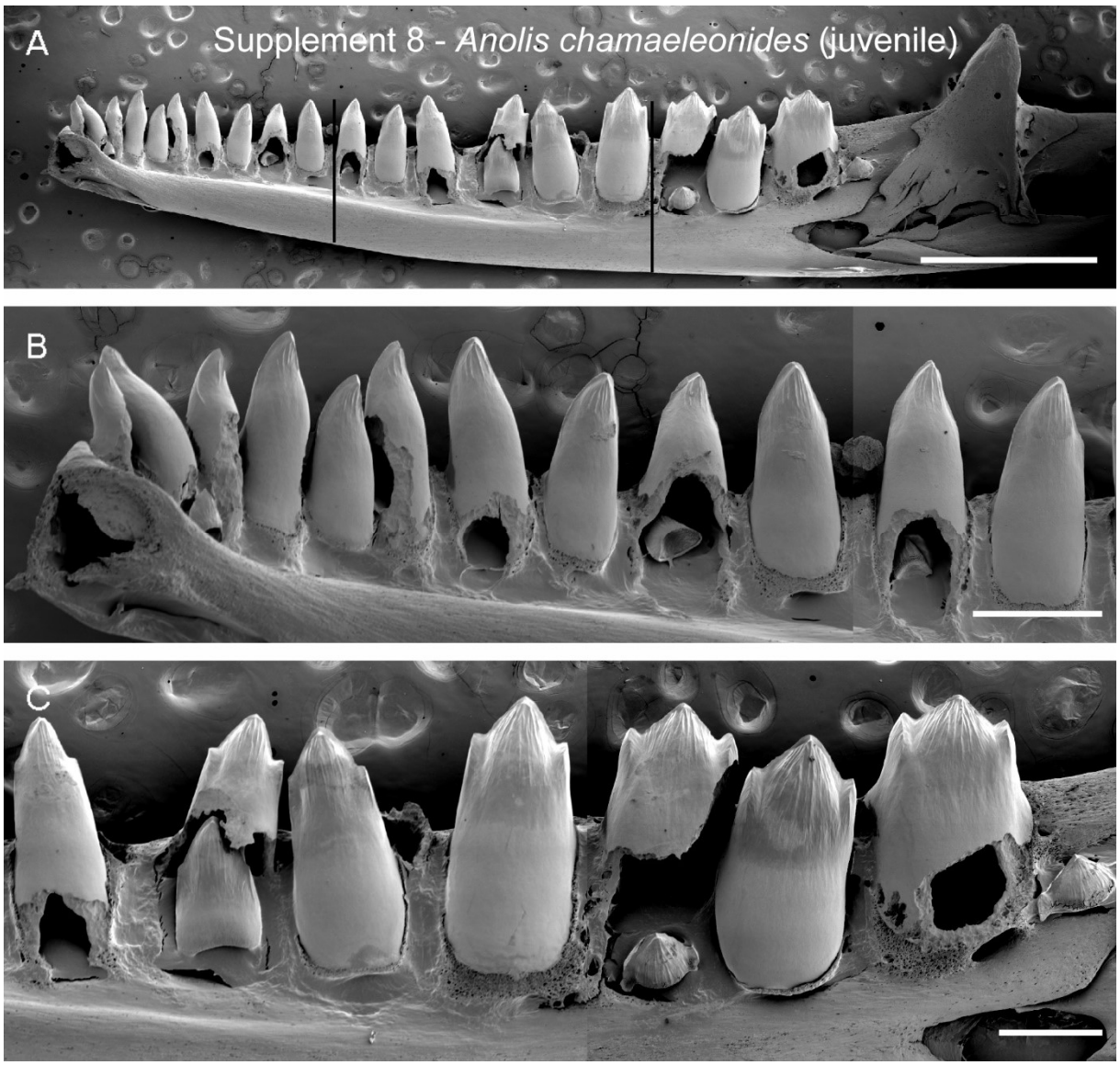


Fig. S8. SEMs of the juvenile dentition of *A. chamaeleonides*. Image (A) shows the lower jaw from the lingual side, with a scale bar of 2 mm. The black vertical lines divide the lower jaw into rostral, middle, and caudal segments. Images (B, C) provide an enlarged view of the dentition, with scale bars of 0.5 mm.

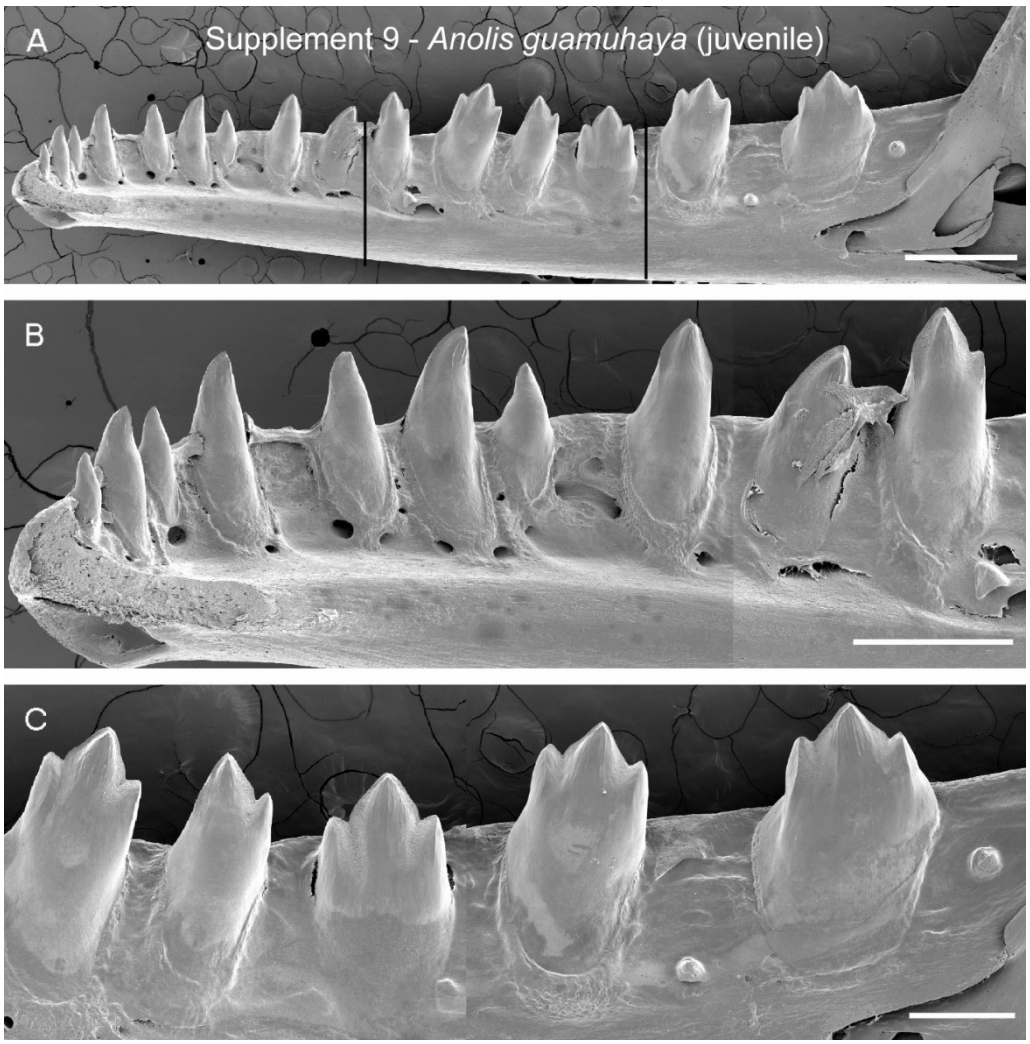


Fig. S9. SEMs of the juvenile dentitions of *A. guamuhaya*. Image (A) shows the lower jaw from the lingual side with a scale bar of 1 mm. The black vertical lines divide the lower jaw into rostral, middle, and caudal segments. Images (B, C) provide an enlarged view of the dentition with scale bars of 0.5 mm.

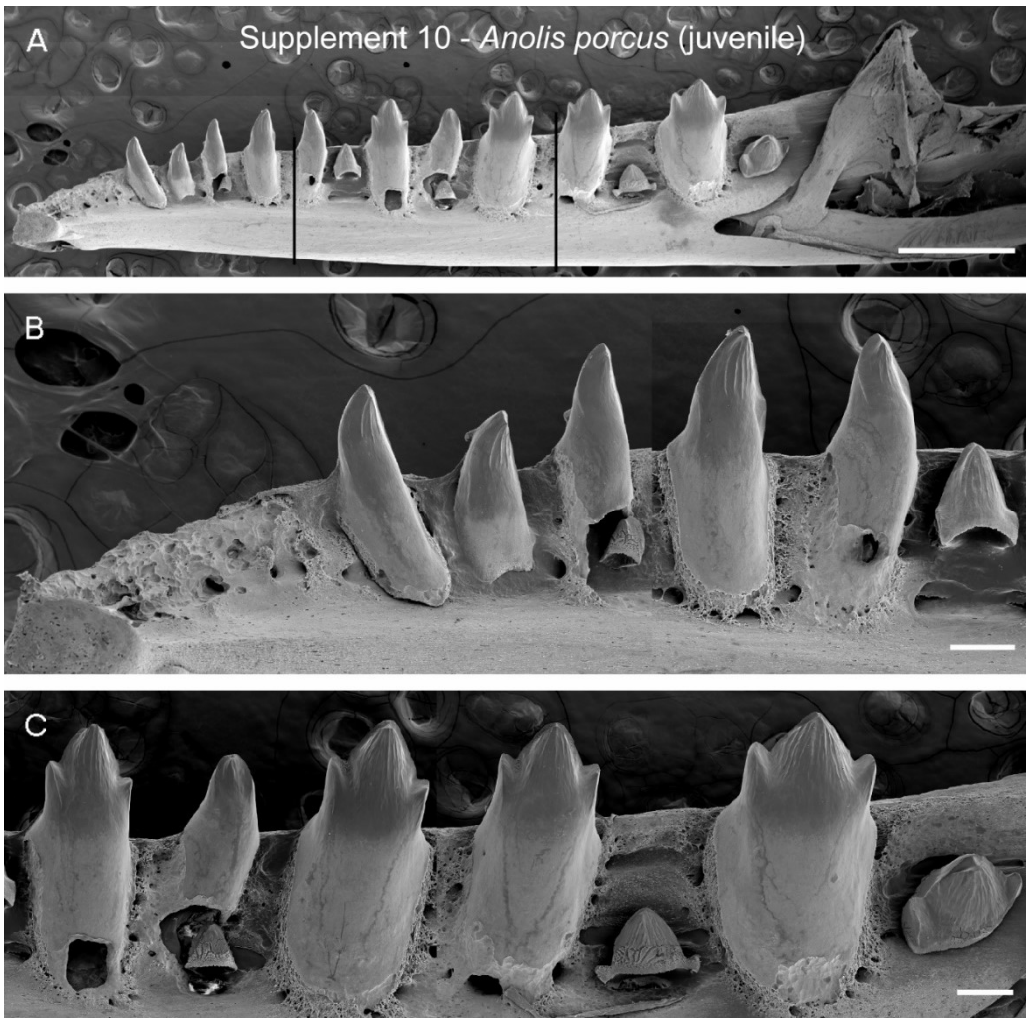


Fig. S10. SEMs of the juvenile dentitions of *A. porcus*. Image (A) shows the lower jaw from the lingual side with a scale bar of 1 mm. The black vertical lines divide the lower jaw into rostral, middle, and caudal segments. Images (B, C) provide an enlarged view of the dentition with scale bars of 0.2 mm.

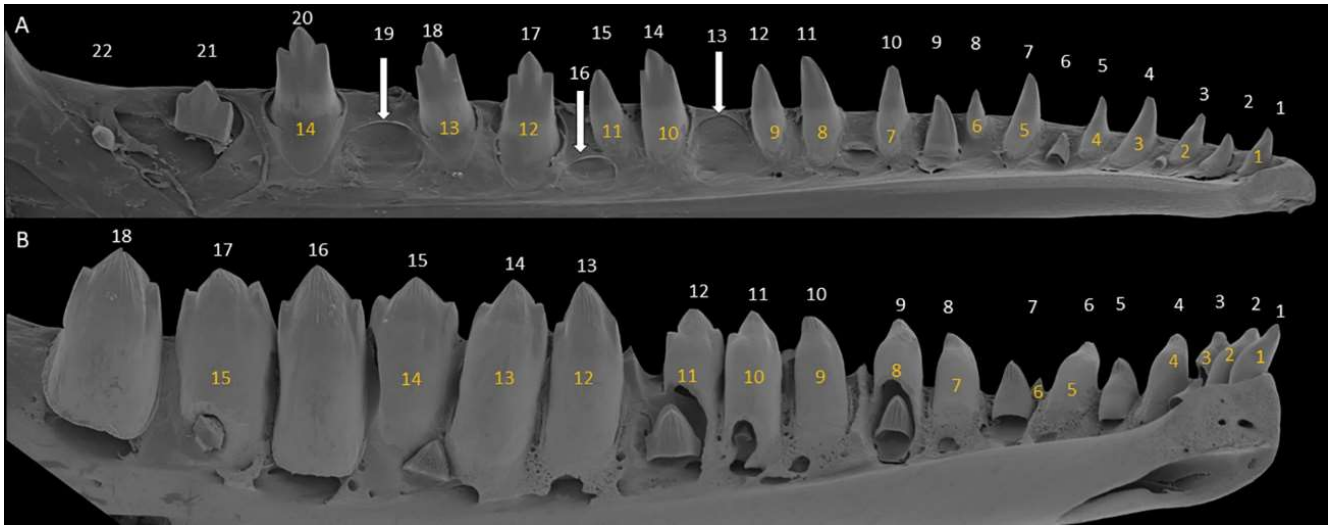


Fig. S11. SEM micrographs showing how tooth positions and the number of ankylosed teeth were counted. Positions and ankylosed teeth were counted from the rostral tip of the jaw. (A) shows the situation in a late embryo, while (B) shows it in a juvenile. White numbers indicate tooth positions, while yellow numbers indicate ankylosed teeth.

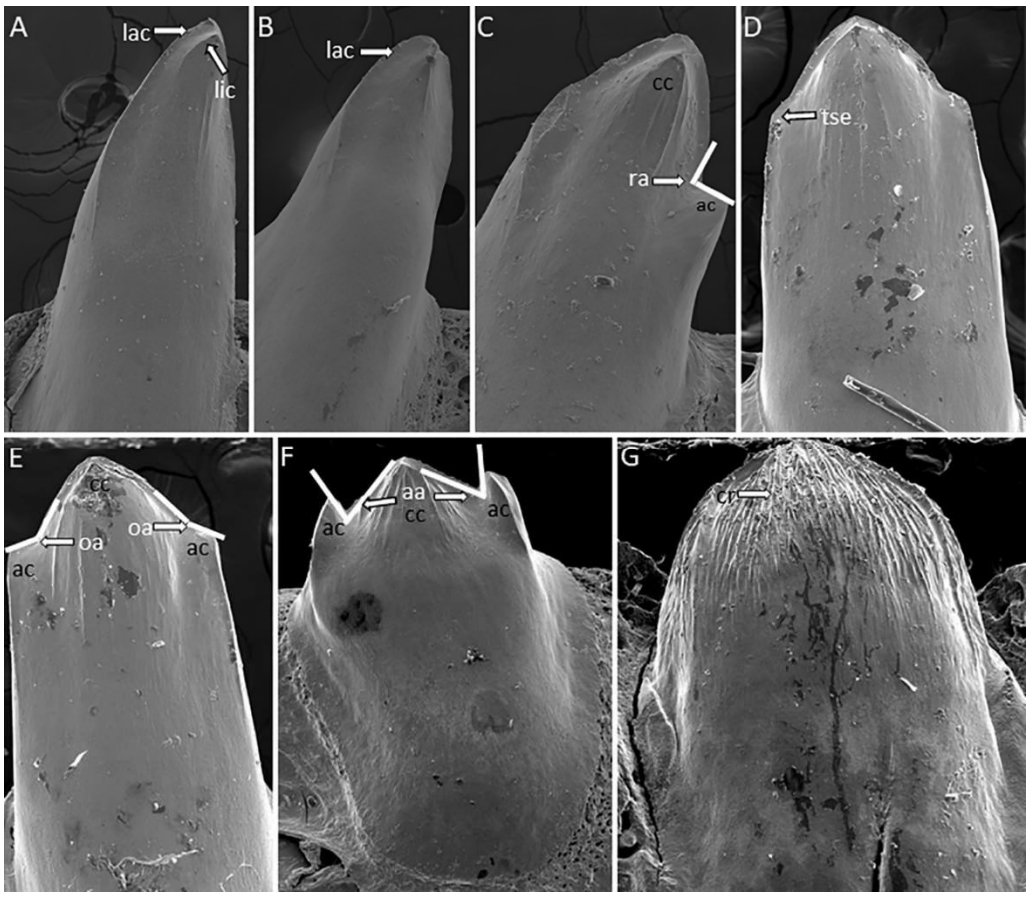


Fig. S12. Figures show tooth shapes and tooth crown features. (A-B and D) depict unicuspid teeth. Unicuspid tooth (A) has a tip divided into labial (lac) and lingual enamel crests (lic), unicuspid tooth (B) shows wear on only the labial enamel crest, and (D) the unicuspid tooth possesses side expansions (tse) that nearly take the shape of accessory cusps. Figure (C) shows a bicuspid tooth with a central cusp (cc) and an accessory cusp (ac) forming a right angle (ra). Figures (E-F) depict tricuspid teeth. The tricuspid tooth in (E) has a central cusp and two accessory cusps forming an obtuse angle (oa), while in (F) the cusps form an acute angle (aa). Figure (G) shows a molariform tooth ornamented with enamel crenulation (cr).

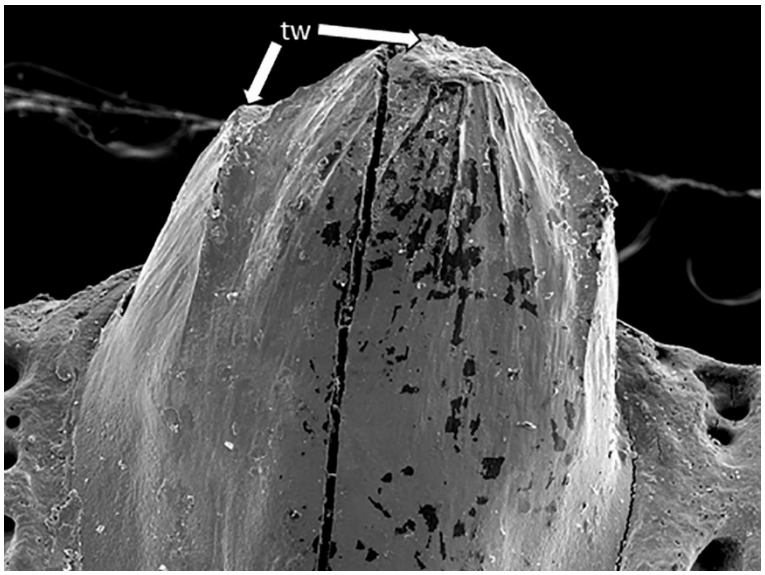


Fig. S13. The figure shows tooth wear (tw). The enamel is damaged in the marked areas of the tooth crown.

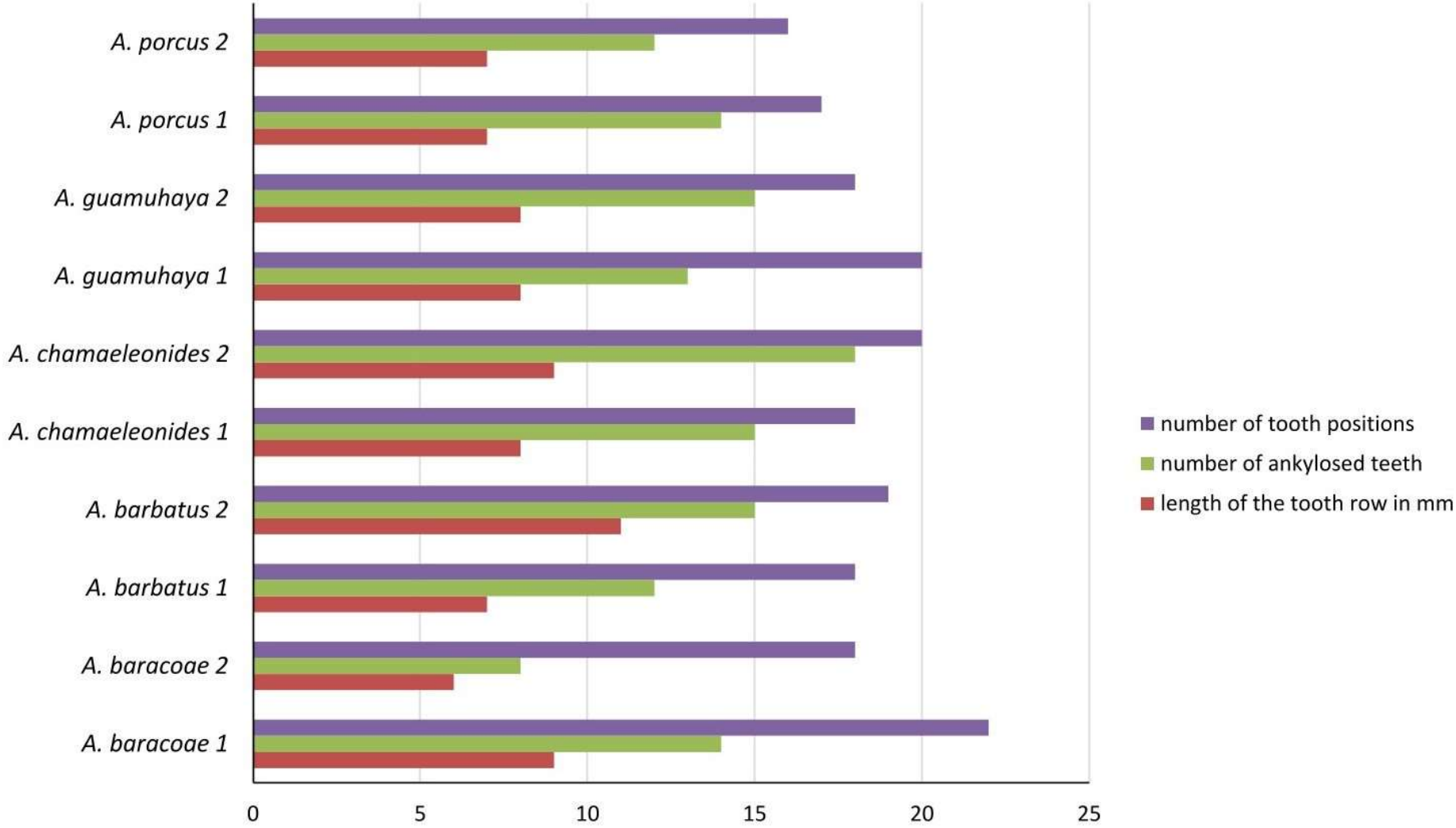


Fig. S14. The chart shows the length of the tooth row, the number of ankylosed teeth, and the number of tooth positions examined in embryos and juveniles.

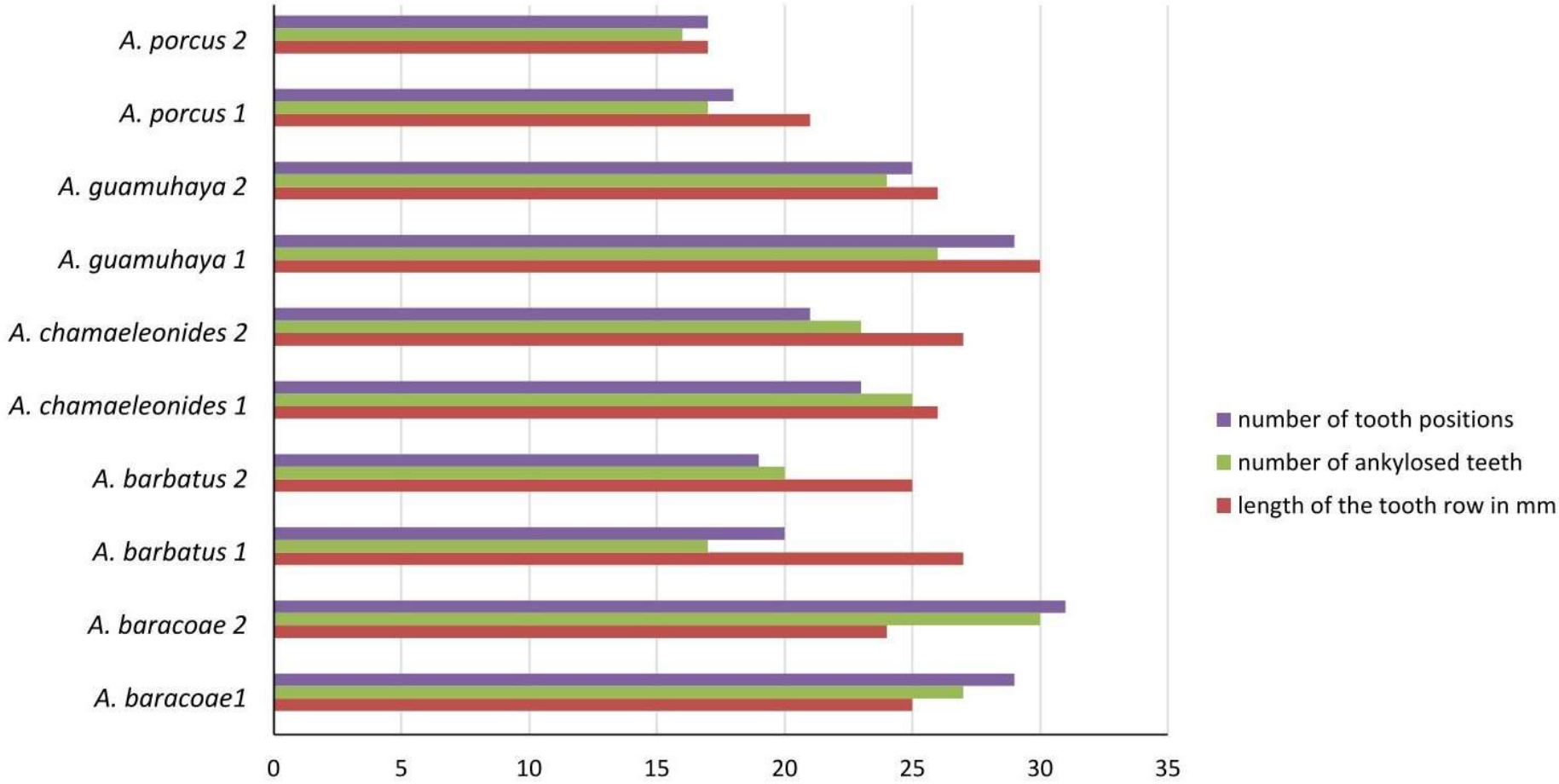


Fig. S15. The chart shows the length of the tooth row, the number of ankylosed teeth, and the number of tooth positions examined in adults.

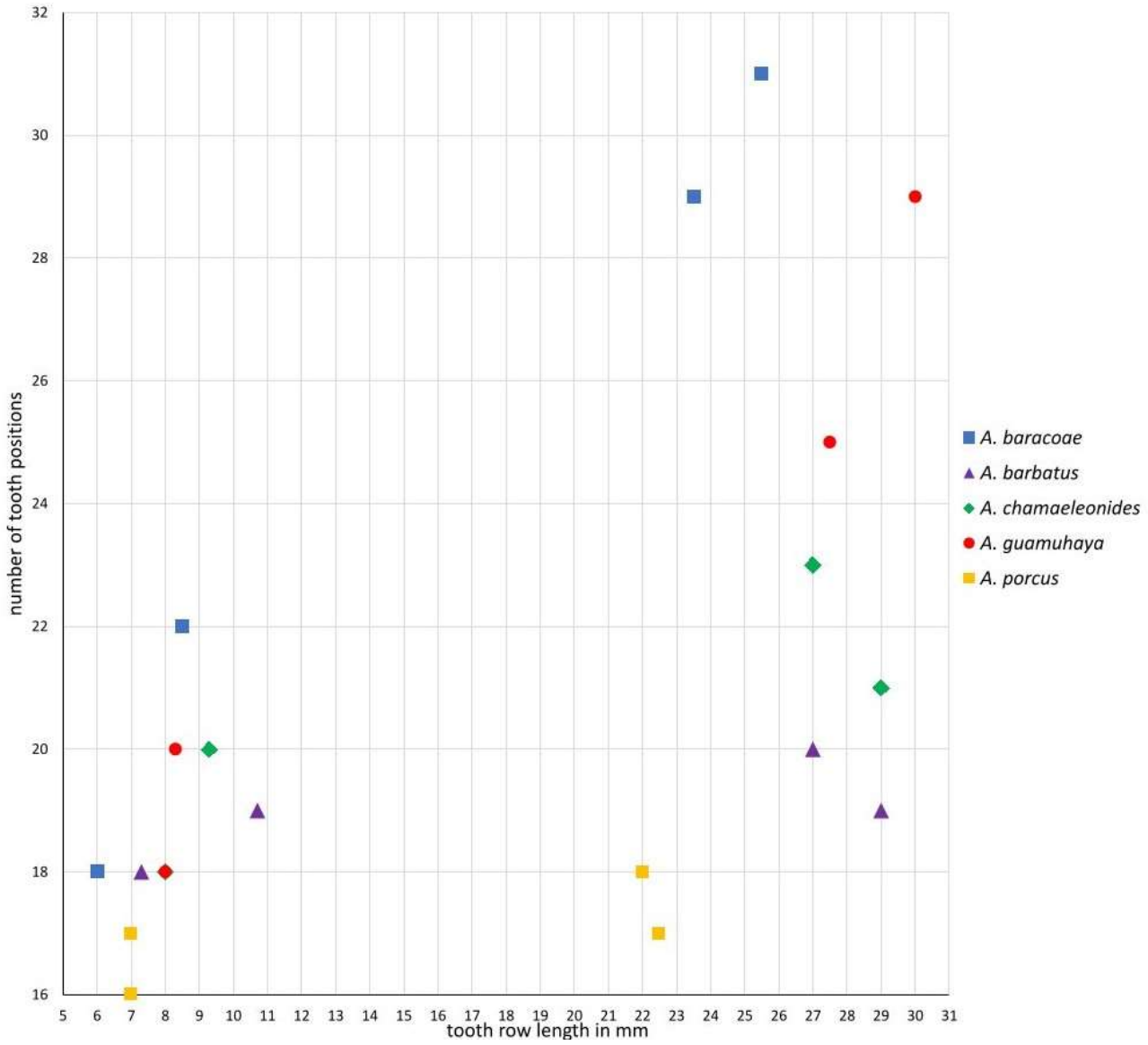


Fig. S16. The chart shows the correlation between the number of tooth positions and the length of the tooth row in the examined anole species.

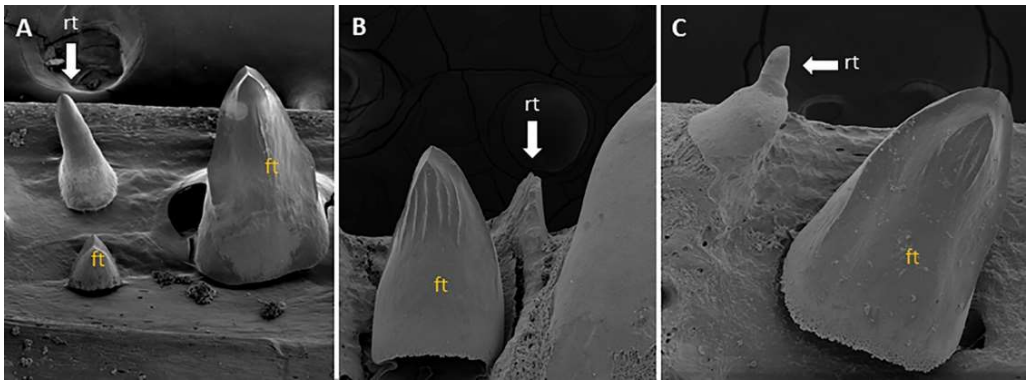


Fig. S17. SEM micrographs show teeth of the rudimentary generation. (A-C) Rudimentary teeth (rt) are miniature mineralized teeth situated between the teeth of the first functional generation (ft).

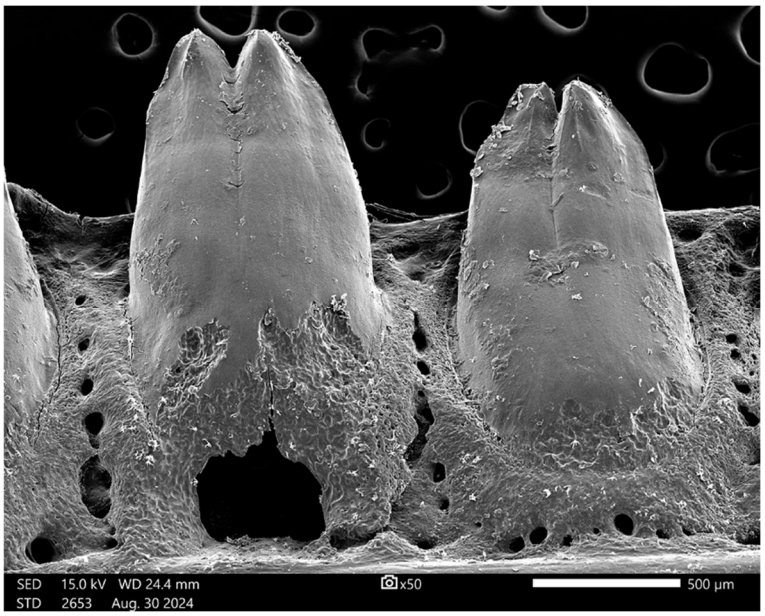


Fig. S18. SEM micrograph shows bicuspid teeth found in one adult *A. baracoae*. These teeth differ from other bicuspid teeth as their cusps are the same size, suggesting the possibility that they formed via the fusion of two tooth germs. This phenomenon has been previously described in egg teeth. In this case, it could be a developmental disorder.

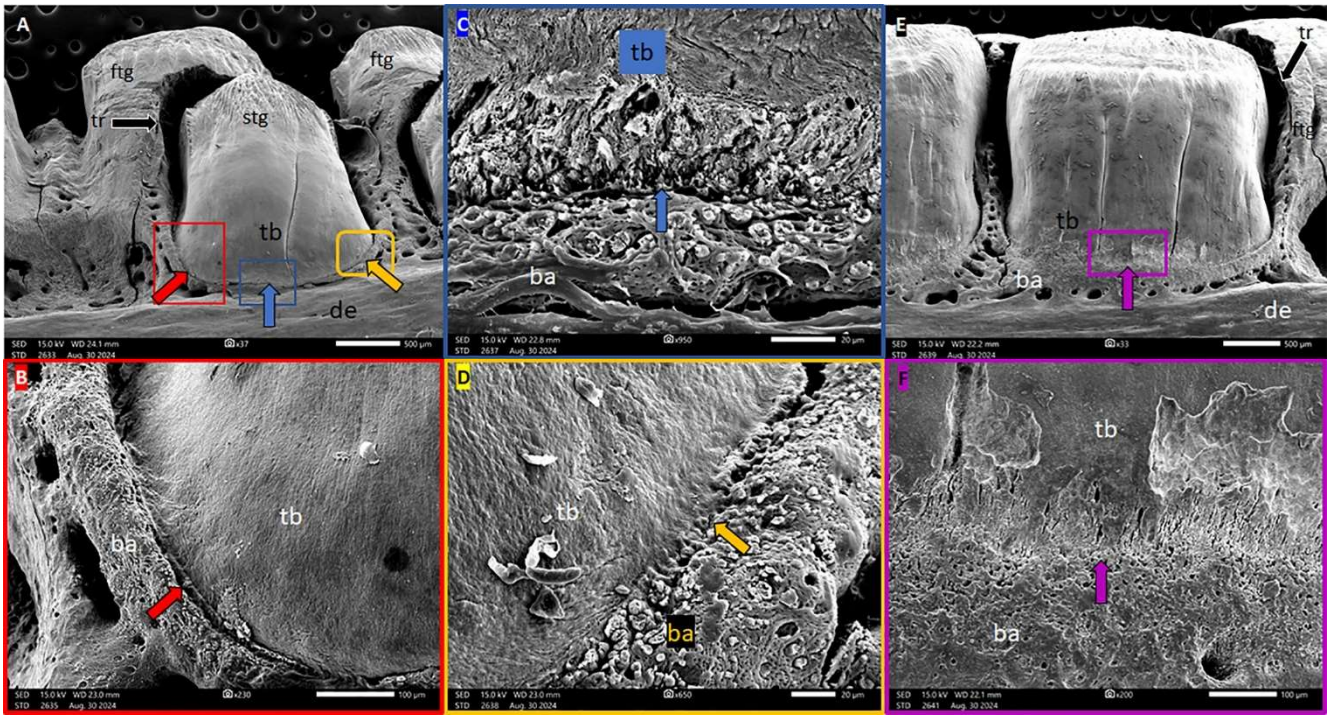


Fig. S19. Shows SEM micrographs of ankylosed teeth that are still growing and those that are no longer growing, attached to the dentale (de) in an adult *A. barbatus*. (A) Shows a still-growing ankylosed tooth (stg) adjacent to a tooth of a former generation (ftg) that is resorbed (tr). (B-D) Provide higher magnification of the tooth base (tb)/bone of attachment (ba) interface, which appears very active in the mineralization process and contributes to positioning the tooth. (E) Shows an ankylosed tooth in its final position. (F) Provides higher magnification of the tooth base/bone of attachment interface, which no longer appears active in the formation of new mineralized tissue.

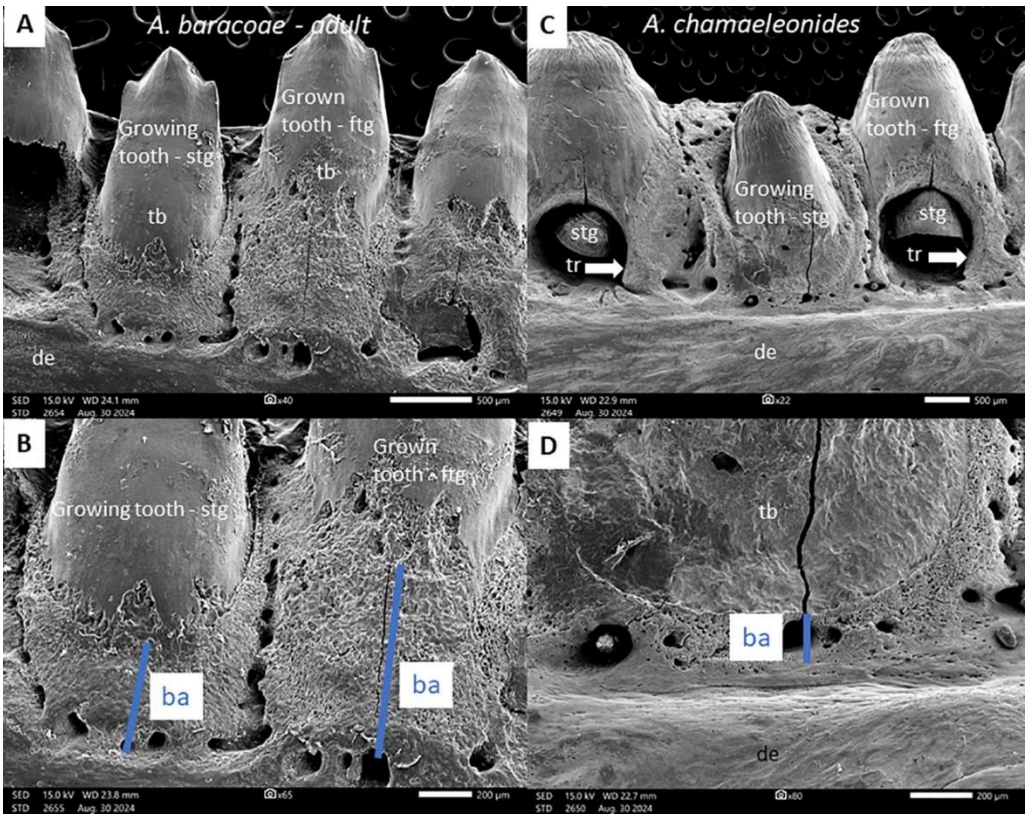


Fig. S20. Shows SEM micrographs of ankylosed teeth that are still growing and those that are no longer growing, attached to the dentale (de) in (A-B) an adult *A. baracoae* and (C-D) *A. chamaeleonides*. (A) Shows a still-growing ankylosed tooth (stg) adjacent to a tooth from a previous generation (ftg). (B) Provides a higher magnification of the tooth base (tb)/bone of attachment (ba) interface in both the still-growing and fully growed teeth. The blue lines mark the width of the bone of attachment. This micrograph clearly shows that the bone of attachment continues to grow after initial ankylosis to shift the tooth into its final position. (C)

Also shows an ankylosed growing tooth next to teeth in their final position, whose tooth bases are already resorbing (tr). Mineralizing teeth of the successive generation (stg) are visible inside the resorbing teeth. (D) Provides a higher magnification of the tooth base/bone of attachment interface in an ankylosed and still-growing tooth. The blue line marks the width of the bone of attachment.

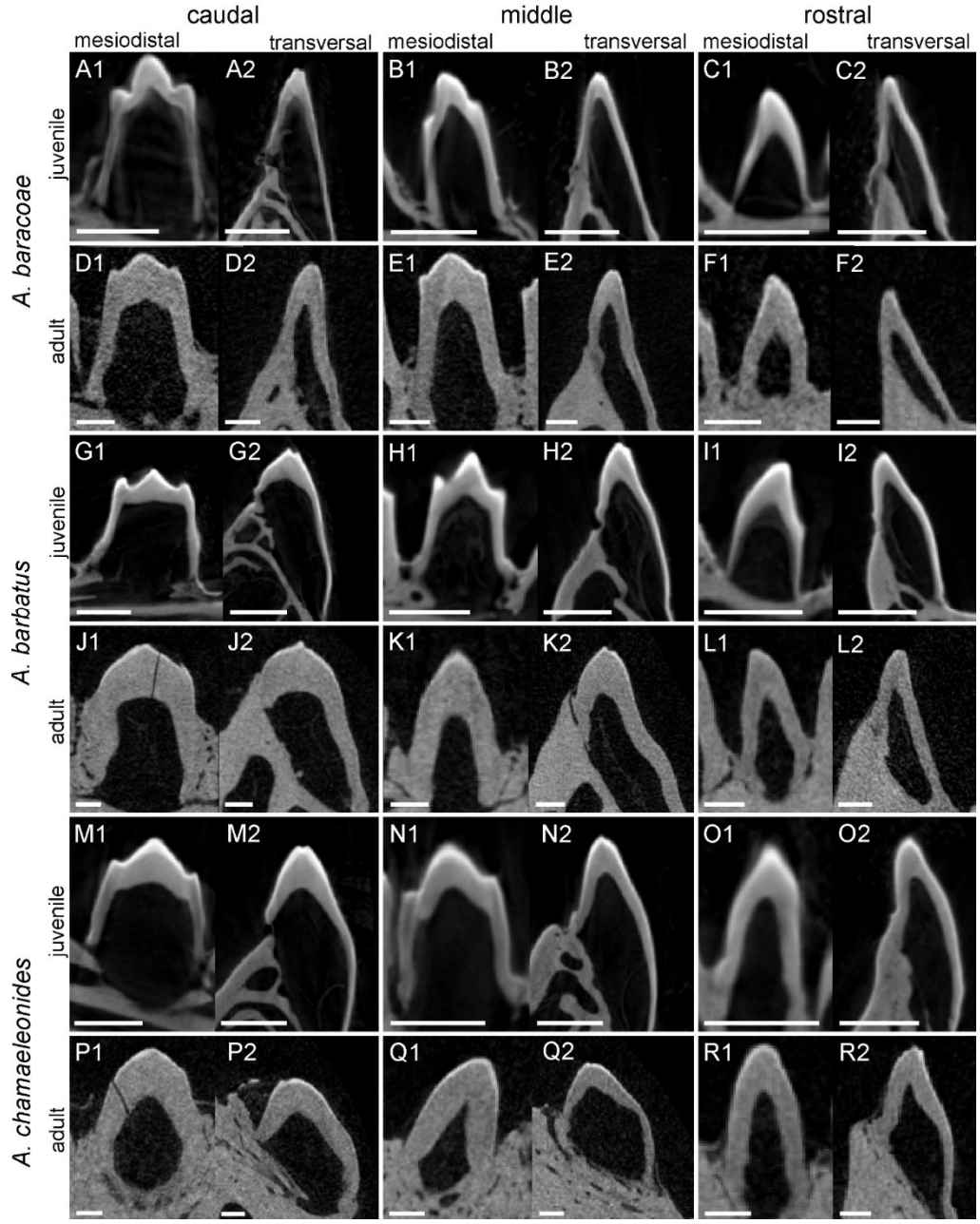


Fig. S21. The figures show micro-CT mesiodistal and transverse sections through selected teeth from the rostral, middle, and caudal segments of the lower jaw in juvenile and adult *A. baracoae*, *A. barbatus* and *A. chamaeleonides*. (A1-F2) depict the dentine deposition in *A. baracoae*, (G1-L2) in *A. barbatus*, and (M1-R2) in *A. chamaeleonides*.

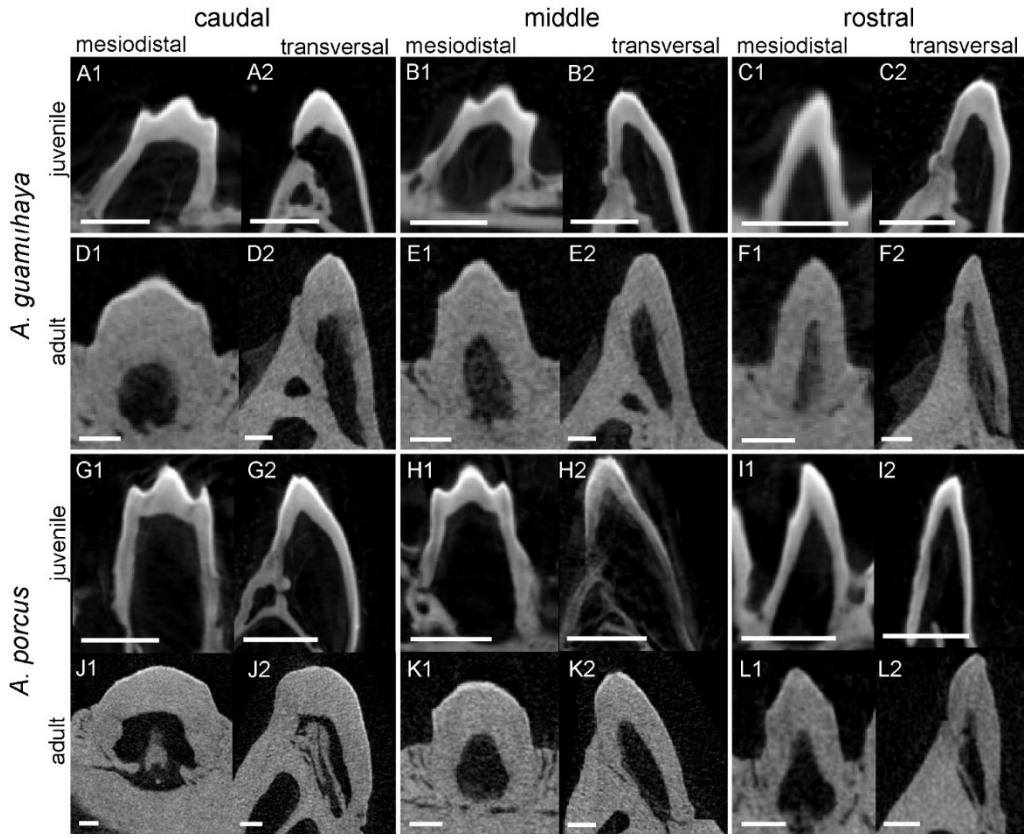


Fig. S22. The figures show micro-CT mesiodistal and transverse sections through selected teeth from the rostral, middle, and caudal segments of the lower jaw in juvenile and adult *A. guamuhaya* and *A. porcus*. (A1-F2) depict the dentine deposition in *A. guamuhaya*, and (G1-L2) in *A. porcus*.